

# Ethylene/Polar Monomer Copolymerization by [N, P] Ti Complexes: Polar Copolymers with Ultrahigh-Molecular Weight

Jingjiao Liu, Jiaojiao Zhang, Min Sun, Hongming Li, Ming Lei,\* and Qigu Huang\*

Cite This: *ACS Omega* 2024, 9, 15030–15039

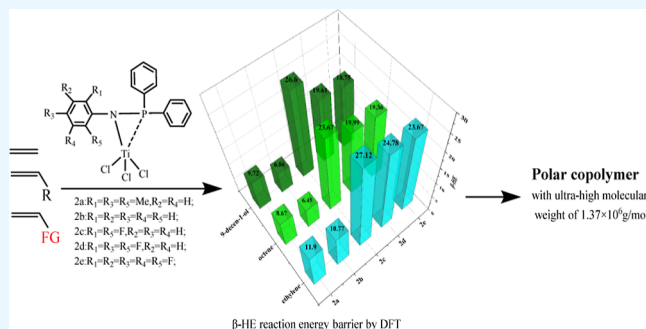
Read Online

ACCESS |

Metrics &amp; More

Article Recommendations

**ABSTRACT:** A series of novel titanium complexes (2a–2e) bearing [N, P] aniline–chlorodiphenylphosphine ligands (1a–1e) featuring CH<sub>3</sub> and F substituents have been synthesized and characterized. Surprisingly, in the presence of polar additive, the complexes (2a–2e) all displayed high catalytic activities (up to  $1.04 \times 10^6$  gPolymer (mol·Ti)<sup>-1</sup>·h<sup>-1</sup>) and produced copolymer with the ultrahigh molecular weight up to  $1.37 \times 10^6$  g/mol. The catalytic activities are significantly enhanced by introducing electron-withdrawing group (F) into the aniline aromatic ring. Especially, the increase in activity based on different complexes followed the order of 2e > 2d > 2c > 2b > 2a. Simultaneously, density functional theory (DFT) calculations have been performed to probe the polymerization mechanism as well as the electronic and steric effects of various substituents on the catalyst backbone. DFT computation revealed that the polymerization behaviors could be adjusted by the electronic effect of ligand substituents; however, it has little to do with the steric hindrance of the substituents. Furthermore, theoretical calculation results keep well in accordance with experimental measurement results. The article provided an appealing design method that the employment of fluorine atom as electron-withdrawing to be studied is the promotive effect of transition-metal coordination polymerization.



## 1. INTRODUCTION

Functional polyolefins have attracted particular attention owing to their excellent comprehensive properties: enhanced surface properties, improved compatibility with other materials, superior printability, dye retention, and degradability.<sup>1–4</sup> The copolymerization of ethylene with polar alkenes should be the most efficient means to functionalized polyethylenes.<sup>1</sup> However, few catalysts for functional polyolefin synthesis exhibited high activity to afford polymers with high molecular weight. Therefore, the acquisition of polar polyolefins with ultrahigh-molecular-weight polar polyolefins remained a significant challenge toward practical application since the catalytic metal active sites were susceptible to poisoning and deactivating by polar functional groups.<sup>5–7</sup>

Up to now, intensive efforts have been devoted to obtaining functionalized polyolefins. Fujita et al.<sup>8</sup> demonstrated that bis(phenoxy-imine) Ti complexes (Ti–FI catalysts) were potent catalysts for ethylene/5-hexene-1-yl-acetate copolymerization, the activity of which was up to  $5.15 \times 10^5$  gPolymer (mol·Ti)<sup>-1</sup>·h<sup>-1</sup> and 0.74 mol % incorporation rate, produced copolymer with  $M_w$  up to  $3.87 \times 10^5$  g/mol. Tang et al.<sup>9</sup> synthesized a series of titanium complexes bearing [O N X] tridentate ligands, the complexes containing sulfur or phosphine donors showed high activity in the copolymerization of ethylene with 9-decen-1-ol up to  $1.3 \times 10^8$  gPolymer (mol·Ti)<sup>-1</sup>·h<sup>-1</sup> with an incorporation rate of up to 8.8 mol %,

and the  $M_w$  of the polymer was  $2.9 \times 10^4$  g/mol. Li et al.<sup>10</sup> developed several well-defined phosphino-phenolate [P, O] neutral nickel catalysts which showed very high catalytic activities for ethylene polymerization even at 90 °C or with the addition of a large amount of a polar additive (such as ethyl alcohol, diethyl ether, acetone, or even water). The polar functional units were mainly incorporated into the polymer main chain and also located at the chain end with insertion percentages of up to 7.4 mol %. Accompanying by the fact that  $M_w$  of the copolymer was  $4.78 \times 10^5$  g/mol in the presence of ethyl acetate. Meanwhile, Li's group<sup>11</sup> reported a bis ( $\beta$ -aminoketone) titanium complex, which can effectively catalyze the copolymerization of ethylene with 5-norbornene-2-methanol with catalytic activity up to  $2.7 \times 10^5$  gPolymer (mol·Ti)<sup>-1</sup>·h<sup>-1</sup> and the  $M_w$  up to  $1.0 \times 10^5$  g/mol. Nozaki et al.<sup>12</sup> exhibited a series of palladium complexes bearing a bisphosphine monoxide with a methylene linker, which successfully catalyze the copolymerization of ethylene and

Received: November 16, 2023

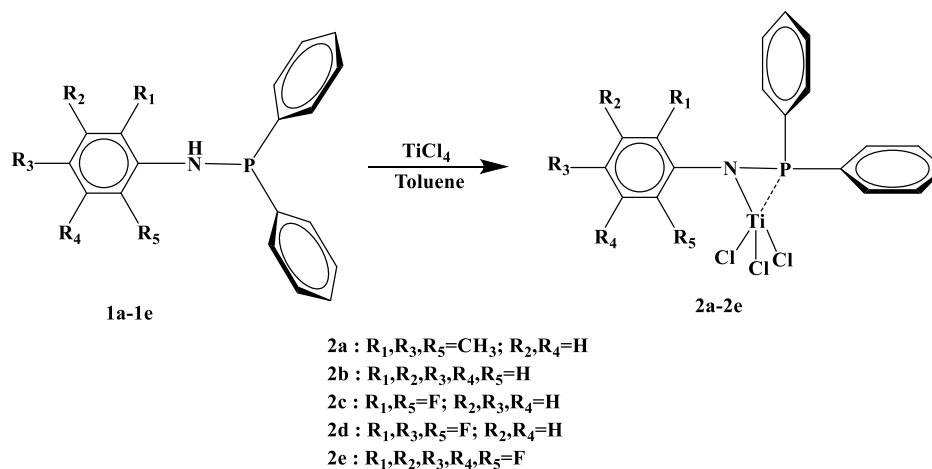
Revised: March 9, 2024

Accepted: March 11, 2024

Published: March 19, 2024



## Scheme 1. Structure and Synthesis of [N, P] Ti Non-metallocene Complexes



various polar monomers such as AAC, DAE, AN, and MMA. The insertion rate AAC monomer can reach 0.72 mol % and the  $M_n$  of the copolymer up to  $4.5 \times 10^3$  g/mol.

Nevertheless, great progress has been made in the development of catalysts to increase the molecular weight of polar polyolefins. To the best of our knowledge, a large amount of financial resources has been invested in the synthesis of catalysts, and the multistep reaction of catalysts was cumbersome, and the synthetic route was complicated. Simultaneously, it was worth noting that the  $M_w$  of the obtained polar olefin copolymer reported in the literature has not reached a satisfactory level, which has become a major obstacle in industrial applications. Rather than previous traditional idea of designing catalysts, our research team adopted the simplest and the most economical direct synthetic approach. Meanwhile, the novel [N, P] Ti-based non-metallocene catalyst we designed and synthesized exhibited high catalytic activity in the presence of polar monomers and the copolymer with ultrahigh molecular weight which was expected to improve the practical industrial application of polar polyolefin. The copolymerization experiment of ethylene and 9-decen-1-ol was carried out for the first time by using 9-decen-1-ol as comonomer. We were pleased to find that the catalyst with high activity ( $1.04 \times 10^6$  gPolymer (mol·Ti) $^{-1}$ ·h $^{-1}$ ), good incorporation ratio of 9-decen-1-ol (1.91 mol %), and the copolymer with the ultrahigh-molecular weight up to  $1.37 \times 10^6$  g/mol. Remarkably, the catalyst highlighted the excellent functional group tolerance of this titanium system. To further understand the structure–reactivity relationship of the catalysts, density functional theory (DFT) calculations were provided to gain insights into the polymerization mechanism.<sup>1,13–15</sup>

## 2. EXPERIMENTAL SECTION

**2.1. Materials.** Mesityl aniline, phenyl aniline, 2,6-difluorophenyl aniline, 2,4,6-trifluorophenyl aniline, 2,3,4,5,6-pentafluorophenyl aniline, chlorodiphenylphosphonium, methyl magnesium chloride, and *n*-butyllithium were purchased from J&K (Beijing, China). 1-octene, 9-decen-1-ol, triethylamine, titanium tetrachloride, and trimethylchlorosilane were provided by Macklin (Shanghai, China). Toluene, *n*-hexane, hydrochloric acid, and absolute ethanol were obtained from Beijing Chemical Factory (Beijing, China). Methyl aluminoxane (MAO, 10 g/100 mL toluene) was bought from Huawei

Ruiké Chemical Co., Ltd. (Beijing, China). Toluene and *n*-hexane solvent were subjected to reflux pretreatment.

**2.2. Synthesis of the Ligand.** All manipulations involving air- and moisture-sensitive compounds were carried out in Schlenk-type glassware under a dry nitrogen atmosphere. The synthesis of the ligands is according to the lectures.<sup>16</sup> Aniline (1.82 mL, 0.02 mol) was injected into Schlenk glassware and was charged with 100 mL of toluene. Methyl magnesium chloride (6.67 mL, 0.02 mol) was then added dropwise to the reaction system under the ice salt environment ( $-10$  °C). Subsequently, chlorodiphenylphosphonium (3.58 mL, 0.02 mol) was then introduced, and the reaction was stirred for 4 h at room temperature. After the desired period of time, the system was filtered under a nitrogen atmosphere, and the supernatant was kept, then distilled under reduced pressure, and washed with *n*-hexane. White powder was obtained in a yield of 87.6%.

**2.3. Synthesis of the Catalyst.** A dry Schlenk glassware was prepared by removing water and oxygen, and then freshly distilled toluene (50 mL) was added. Then, the weighed ligand (1.00 g, 3.60 mmol) was added into the glassware, and the mixture was stirred to ensure that the ligand could be completely soluble in toluene. Subsequently, *n*-butyl lithium (1.50 mL, 2.40 M/L) was added dropwise to the reaction system, and the reaction was continued for 3 h in an ice salt bath environment ( $-10$  °C). Similarly, titanium tetrachloride (0.69 g, 3.60 mmol) was also added dropwise, and the mixture was stirred for 1 h under an ice bath environment ( $-10$  °C). Then, the temperature was gradually increased to 50 °C, and the reaction was continued for 4 h. After the reaction was over, the precipitates were filtered and washed with toluene. The solvent was moved from the filtrate by vacuum. Red solid powder was obtained with 1.2 g and a yield of 81.2%. The schematic diagram of catalyst synthesis is shown in Scheme 1. The characterization and yields in % and in grams of the ligands and Ti complexes were supported in the Supporting Information. The synthesis and the structure characterization of the compounds and Ti complexes are according to the patent<sup>16</sup> and the lectures.<sup>17–19</sup>

**2.4. (Co)Polymerization Procedures.** All of the polymerization processes were carried out in Schlenk-type glassware, which was evacuated for all moisture and oxygen. Toluene (100 mL), catalyst ( $2 \times 10^{-5}$  mol), and MAO cocatalyst were added into the reactor successively under a high purity

nitrogen atmosphere at room temperature. Subsequently, the reaction flask was heated to 60 °C and charged with ethylene (0.05 MPa), and the mixture was stirred for 5 min. At the end of the reaction, the catalytic solution was quenched by the addition of HCl/ethanol solution (3:7 v/v). After being filtered and washed several times with ethanol, the polymer was dried under vacuum at 60 °C until it achieved a constant weight.

**2.5. Characterization.** Structural characterization of the ligand was determined by  $^1\text{H}$  NMR (400 MHz, Bruker, Germany) at room temperature, using  $\text{CDCl}_3$  as the solvent.  $^1\text{H}$  NMR and  $^{13}\text{C}$  NMR characterization of polymers were detected at 120 °C (500 MHz, Bruker, Germany), using a mixed solution (1:1 by volume) of *o*-dichlorobenzene and deuterated *o*-dichlorobenzene as the solvent. The molecular weight of the ligand was detected by mass spectrometry (GSD301, Pfeiffer, Germany), using acetonitrile as dissolvent. The functional groups of the polymer were characterized by Fourier-transform infrared (Nicolet 6700, Thermo Company, USA) with id3 accessory, and the scanning range of the spectrum was 400–4000  $\text{cm}^{-1}$ . The molecular weight of the polymer was determined by GPC (PL-GPC200, Polymer laboratories, UK) at 150 °C. The sample preparation solvent is trichlorobenzene.

**2.6. Computational Details.** All DFT calculations were performed with the Gaussian 09 program.<sup>20</sup> The geometry optimization and frequency calculations were carried out using the WB97XD/B3LYP hybrid exchange–correlation functional. The 6-31G\* basis set was used for H, C, N, P, Si, F, and O atoms, and the LanL2DZ basis set was used for the Ti atom. As shown in previous studies, such functional and basis sets have been fully tested and proven to be reliable. The transition states were ascertained by a single imaginary frequency for the correct mode.<sup>21</sup>

### 3. RESULTS AND DISCUSSION

A series of [N, P] Ti nonmetallocene complexes with different substituents on the aromatic ring were synthesized [2a–2e, mesityl, phenyl, 2,6-difluorophenyl (or 2,6-F2-Ph), 2,4,6-trifluorophenyl (or 2,4,6-F3-Ph), and 2,3,4,5,6-pentafluorophenyl (or 2,3,4,5,6-F5-Ph)-diphenyl phosphine trichlorotitanium, Scheme 1] and applied for olefin copolymerization under atmospheric pressure.<sup>16,19</sup> The representative polymerization results are summarized in Tables 1–4.

**3.1. Ethylene Homopolymerization.** First, the ethylene homopolymerization under different  $n(\text{Al})/n(\text{Ti})$  ratios using complexes 2a–2e was investigated (Table 1). All complexes exhibited very high activity, among which the activity of complex 2e was as high as  $3.68 \times 10^6$  g Polymer  $(\text{mol}\cdot\text{Ti})^{-1}\cdot\text{h}^{-1}$ . Along with an increase from 450 to 650 of the  $n(\text{Al})/n(\text{Ti})$  ratios, the catalytic activity of complexes increased to reach the maximum activity and then decreased gradually [2a: 450 vs 550 vs 650 =  $3.04$  vs  $3.20$  vs  $3.11 \times 10^6$  gPolymer  $(\text{mol}\cdot\text{Ti})^{-1}\cdot\text{h}^{-1}$ ]. Simultaneously, the complexes exhibited the highest activity when the  $n(\text{Al})/n(\text{Ti})$  ratio was 550. It can be seen that the activity of the complexes can be regulated by adjusting  $n(\text{Al})/n(\text{Ti})$  ratios; the increase of  $n(\text{Al})/n(\text{Ti})$  ratios could have a negative effect on the catalytic activity. The less the amount of MAO added, the active center was easy to be destroyed by impurities, and the more the amount of MAO added, the more favorable the transfer of the active center to TMA in MAO.<sup>22–24</sup>

**Table 1. Complexes 2a–2e for Ethylene Homopolymerization under Different  $n(\text{Al})/n(\text{Ti})$  Ratios**

entry	complex	$n(\text{Al})/n(\text{Ti})$	$A^a(\times 10^6)$	$M_w^b(\times 10^5)$	$M_w/M_n^b$
1	2a	450	3.04	7.7	2.35
2		550	3.20	7.4	2.39
3		650	3.11	6.7	2.44
4	2b	450	3.12	8.9	2.42
5		550	3.35	7.8	2.45
6		650	2.48	6.4	2.61
7	2c	450	3.21	11.5	2.65
8		550	3.44	13.9	2.50
9		650	3.36	11.7	2.32
10	2d	450	3.32	11.3	2.59
11		550	3.55	14.4	2.47
12		650	3.41	12.0	2.39
13	2e	450	3.45	13.5	2.52
14		550	3.68	14.9	2.49
15		650	3.54	13.2	2.62

<sup>a</sup>Catalytic activity: gPolymer  $(\text{mol}\cdot\text{Ti})^{-1}\cdot\text{h}^{-1}$ . <sup>b</sup>Determined by GPC, g/mol. Polymerization conditions, complexes:  $2 \times 10^{-5}$  mol; ethylene pressure: 0.05 MPa; temperature: 60 °C; toluent: 100 mL; time: 5 min.

**Table 2. Complexes 2a–2e for Ethylene Homopolymerization**

entry	complex	$T$ (°C)	$A^a(\times 10^6)$	$M_w^b(\times 10^5)$	$M_w/M_n^b$
16	2a	40	2.06	8.0	3.05
17		60	3.20	7.4	3.39
18		80	1.77	6.4	3.24
19	2b	40	2.15	8.4	3.69
20		60	3.35	7.8	3.45
21		80	1.73	6.7	3.04
22	2c	40	2.22	12.1	3.34
23		60	3.44	13.9	3.59
24		80	1.97	12.7	4.28
25	2d	40	2.31	13.2	3.55
26		60	3.55	13.5	4.14
27		80	2.02	12.4	3.78
28	2e	40	2.54	13.6	3.54
29		60	3.68	14.9	3.49
30		80	2.15	13.9	4.69

<sup>a</sup>Catalytic activity: gPolymer  $(\text{mol}\cdot\text{Ti})^{-1}\cdot\text{h}^{-1}$ . <sup>b</sup>Determined by GPC, g/mol. Polymerization conditions, complex:  $2 \times 10^{-5}$  mol; ethylene pressure: 0.05 MPa; toluent: 100 mL; time: 5 min.

Second, the catalytic ability of complexes 2a–2e also was influenced by the reaction temperature significantly, and the ethylene homopolymerization under different temperature (40–80 °C) was also investigated in detail (Table 2). These results exhibited that complexes bearing F (2c, 2d, and 2e) are more active than the complexes bearing  $\text{CH}_3$ , H (2a, 2b). Additionally, ethylene homopolymerization reactions conducted at 60 °C were significantly more productive in comparison to 40/80 °C reactions (2e: 40 vs 60 vs 80 °C =  $2.54$  vs  $3.68$  vs  $2.15 \times 10^6$  gPolymer  $(\text{mol}\cdot\text{Ti})^{-1}\cdot\text{h}^{-1}$ ). The  $M_w$  values observed for experiments using 2d and 2e are obviously higher than those complexes 2a, 2b, and 2c. The molecular weight varied in the order 2e > 2d > 2c > 2b > 2a. Temperature-dependence studies revealed that the polymerization temperature was an important factor affecting the catalytic performance of the complexes. Before reaching the optimal temperature, the higher the temperature, the higher

Table 3. Complexes 2a–2e for Copolymerization of Ethylene and 1-Octene

entry	complexes	octene (mL)	$A^a(\times 10^6)$	octene <sup>b</sup> (mol %)	$M_w^c(\times 10^5)$	$M_w/M_n^c$	$T_m^e$ (°C)
31	2b	5	3.00	3.00	7.50	2.78	126.1
32		10	2.97	3.10	7.70	3.04	124.2
33		15	2.79	4.24	7.00	3.24	121.1
34	2a	10	2.96	3.17	6.81	3.47	123.5
35	2c	10	3.00	3.20	10.01	3.15	123.2
36	2d	10	3.10	3.29	12.13	3.77	122.6
37	2e	10	3.22	3.52	13.16	3.90	121.5

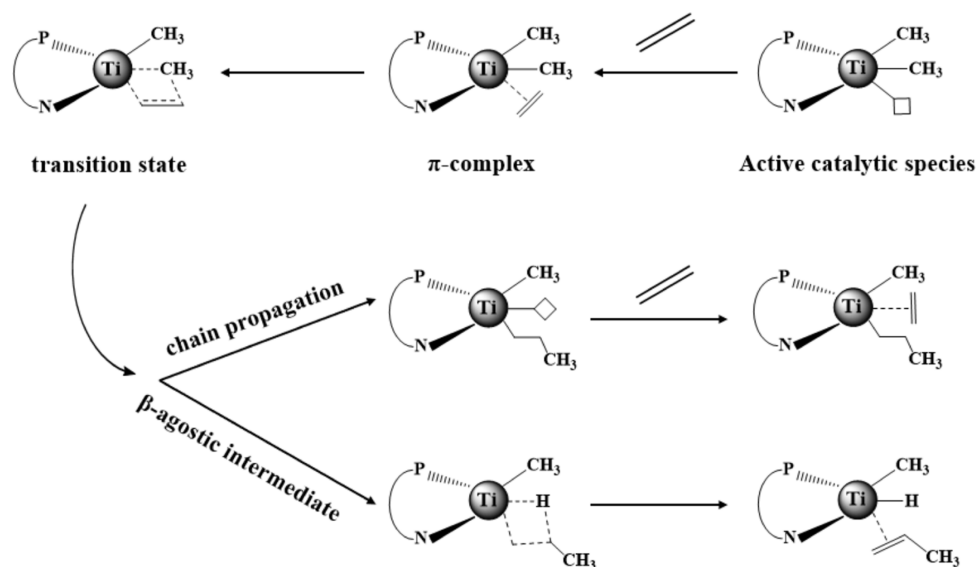
<sup>a</sup>Catalytic activity: gPolymer (mol·Ti)<sup>-1</sup>·h<sup>-1</sup>. <sup>b</sup>Determined by <sup>13</sup>C NMR. <sup>c</sup>Determined by GPC, g/mol. Polymerization conditions: concentration of catalyst:  $2 \times 10^{-5}$  mol; ethylene pressure: 0.05 MPa;  $n(\text{Al})/n(\text{Ti}) = 550$ ; temperature: 60 °C; toluent: 100 mL; time: 5 min.

Table 4. Copolymerization of Ethylene, 1-Octene, and 9-Decen-1-ol<sup>a</sup>

entry	complexes	$A^b(\times 10^6)$	9-decen-1-ol (mol %) <sup>c</sup>	1-octene (mol %) <sup>c</sup>	$M_w^d(\times 10^5)$	$M_w/M_n^d$	$T_m^e$ (°C)
38	2a	0.79	1.31	3.38	5.1	4.4	119.1
39	2b	0.86	1.23	3.18	6.1	4.9	118.6
40	2c	0.93	1.73	4.46	10.2	5.1	118.4
41	2d	0.96	1.79	4.61	11.3	5.5	118.7
42	2e	1.04	1.70	4.38	13.7	5.7	118.2

<sup>a</sup>Polymerization conditions: catalyst:  $2 \times 10^{-5}$  mol; cocatalyst MAO: Al/Ti = 550; toluene: 100 mL; time: 5 min; temperature: 60 °C; ethylene pressure: 0.05 MPa; 1-octene: 10 mL; 9-decen-1-ol: 2 mL, treated by Me<sub>3</sub>SiCl before use. <sup>b</sup>gPolymer (mol Ti)<sup>-1</sup>·h<sup>-1</sup>. <sup>c</sup>Determined by <sup>1</sup>H, <sup>13</sup>C NMR spectra. <sup>d</sup>Molecular weight and dispersity were determined by GPC. <sup>e</sup> $T_m$ : determined by DSC.

Scheme 2. Possible Mechanism Diagram for Ethylene Polymerization



the activity and the faster the rate of polymerization growth. Exceeding the optimum temperature and continuing to heat up, the catalyst structure was unstable and decomposed. The result indicates that the catalysts of 2c, 2d, and 2e are stable to the temperature because of the strong electron-withdrawing groups F substituted in ligands.

**3.2. Ethylene/1-Octene Copolymerization.** To gain further insights into the copolymerization performance of the complexes 2a–2e, the copolymerization for ethylene/1-octene was explored. Furthermore, the corresponding results are compiled in Table 3. 1-Octene was used as a comonomer to investigate the copolymerization behavior of the complexes. Complexes 2a–2e produced copolymers with enhanced comonomer contents (3.0–4.24%). Increasing the amount of 1-octene resulted in higher incorporation (entries 31–33). Analysis data of copolymerization indicated that complexes

bearing F group (2e) induced higher comonomer incorporation than the CH<sub>3</sub> group (2a). There is an obvious relationship between the molecular weight and the nature of the substituent. The introduction of electron-withdrawing group (F) resulted in a higher-molecular weight (2e:13.16 g/mol), whereas the introduction of electron-donating group (CH<sub>3</sub>) lead to a lower-molecular weight (2a:6.81 g/mol). The results displayed that the complexes exhibited high-efficiency copolymerization.

**3.3. Ethylene/1-Octene/9-Decen-1-ol Copolymerization.** The results of copolymerization of ethylene/1-octene/9-decen-1-ol are summarized in Table 4. The complexes (2a–2e) all displayed high catalytic activities [up to  $1.04 \times 10^6$  gPolymer (mol·Ti)<sup>-1</sup>·h<sup>-1</sup>] and produced copolymer with the ultrahigh-molecular weight (up to  $1.37 \times 10^6$  g/mol). Simultaneously, the catalysts showed remarkable difference in

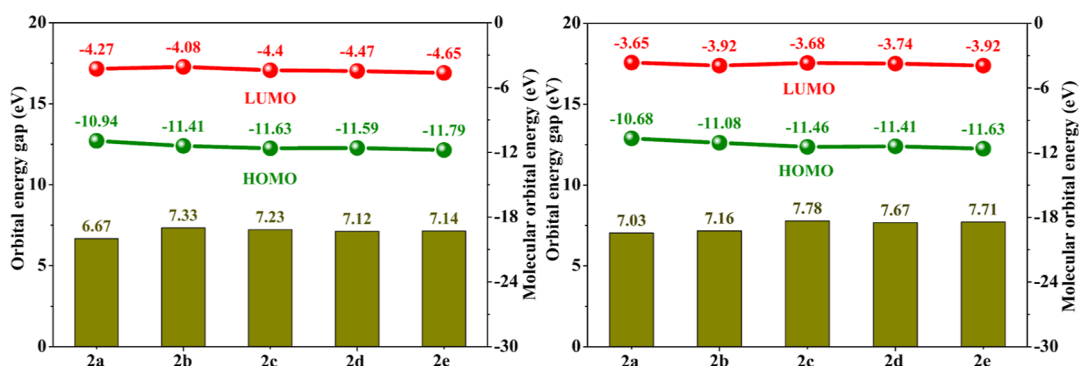


**Figure 1.** HOMO energy, LUMO energy, and the HOMO–LUMO gaps of the frontier molecular orbitals of complexes (2a–2e) and b the active centers (2a–2e) that have initiated the first step of the ethylene reaction.

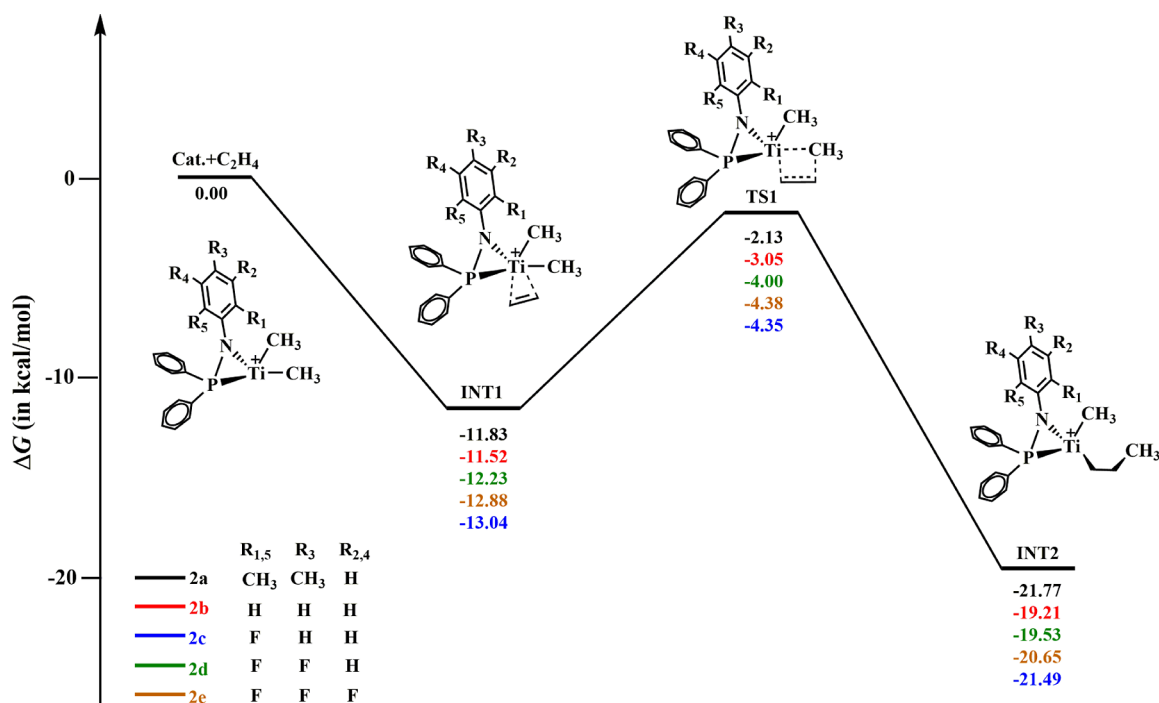


**Figure 2.** Computed energy profiles (free energy in kcal/mol) for insertion of the first ethylene monomer into complexes.

the polymerization activity [varied from 0.79 to  $1.04 \times 10^6$  gPolymer (mol·Ti)<sup>-1</sup>·h<sup>-1</sup>]. We can see that the introduction of fluorine atoms had a more pronounced impact on the polymerization activity compared to that of the CH<sub>3</sub> substituent. Simultaneously, when the number of fluorine increased, the activity was greatly affected, and the sequence of the catalyst capability is 2e > 2d > 2c > 2b > 2a.

To gain more insights into the [N, P] Ti complex-promoted copolymerization, DFT mechanistic analysis was carried out to estimate the state energy and energy barrier.<sup>25</sup> The pictorial representation for [N, P] nonmetallocene complexes to catalyze olefin polymerization is shown briefly in Scheme 2. The active catalytic species possesses a vacant coordination site, which is favorable for complexation of olefin to form a  $\pi$ -complex. Following, the four-membered cyclic transition state was formed between the alkene double bond and the metal–CH<sub>3</sub> bond, which further initiated the polymerization process. Similarly, the newly formed species possesses a vacant coordination site which can serve as the starting point again to ensure that chain propagation can proceed successfully. The proposed mechanism for chain termination is  $\beta$ -hydrogen

elimination, in which the hydrogen atom is transferred to the metal by an agostic interaction. Finally, a vinyl-terminated polymer chain and a catalyst hydride complex were produced via a four-member cyclic transition state.

Complexes with highest occupied molecular orbital (HOMO), lowest unoccupied molecular orbital (LUMO), and energy gaps (HOMO–LUMO) have been extensively studied.<sup>26,27</sup> The stability of complexes (2a–2e) composed of different substituents on ligands (1a–1e) was evaluated in terms of their HOMO–LUMO gaps because the energy difference has a crucial effect on the stability of catalysts. The complexes with smaller HOMO–LUMO gaps indicate more instability and feasible charge transfer. Figure 1 shows HOMO energy, LUMO energy, and the HOMO–LUMO gaps of the Frontier molecular orbital of complexes (2a–2e). It can be observed that HOMO and LUMO energies of 2c–2e are smaller than 2a, which is due to the electron-withdrawing nature of F attached to the ligand (1c–1e). 2c–2e with lower HOMO and LUMO energy presents the better structural stability. The 2a exhibited the lowest HOMO–LUMO gap, indicating that 2a can perform a more feasible charge transfer

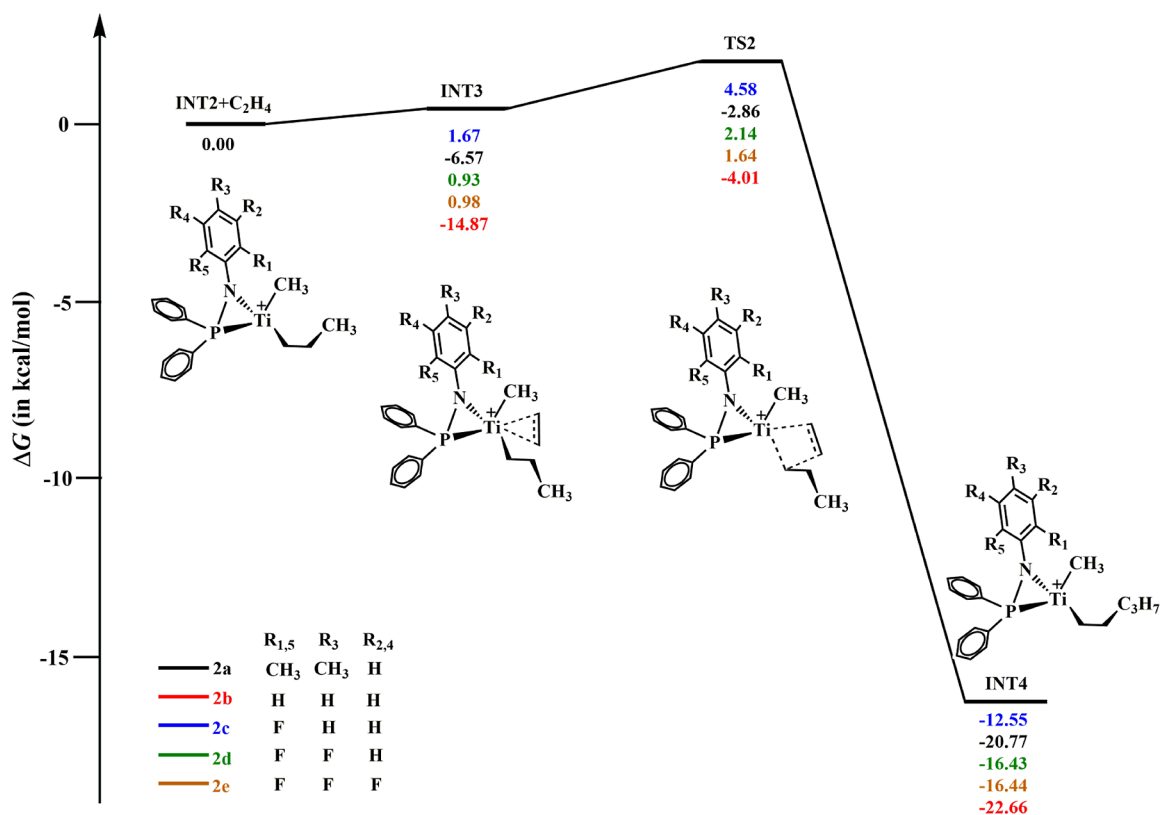


Figure 3. Computed energy profiles (free energy in kcal/mol) for insertion of a second ethylene monomer into INT2.

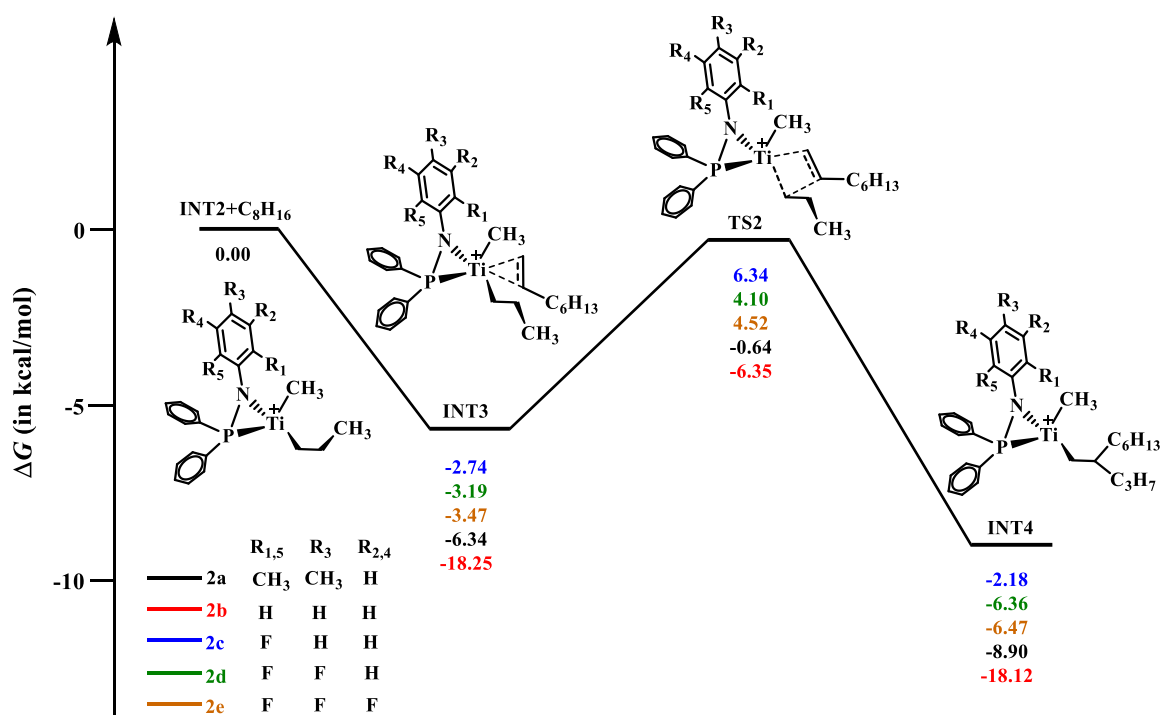
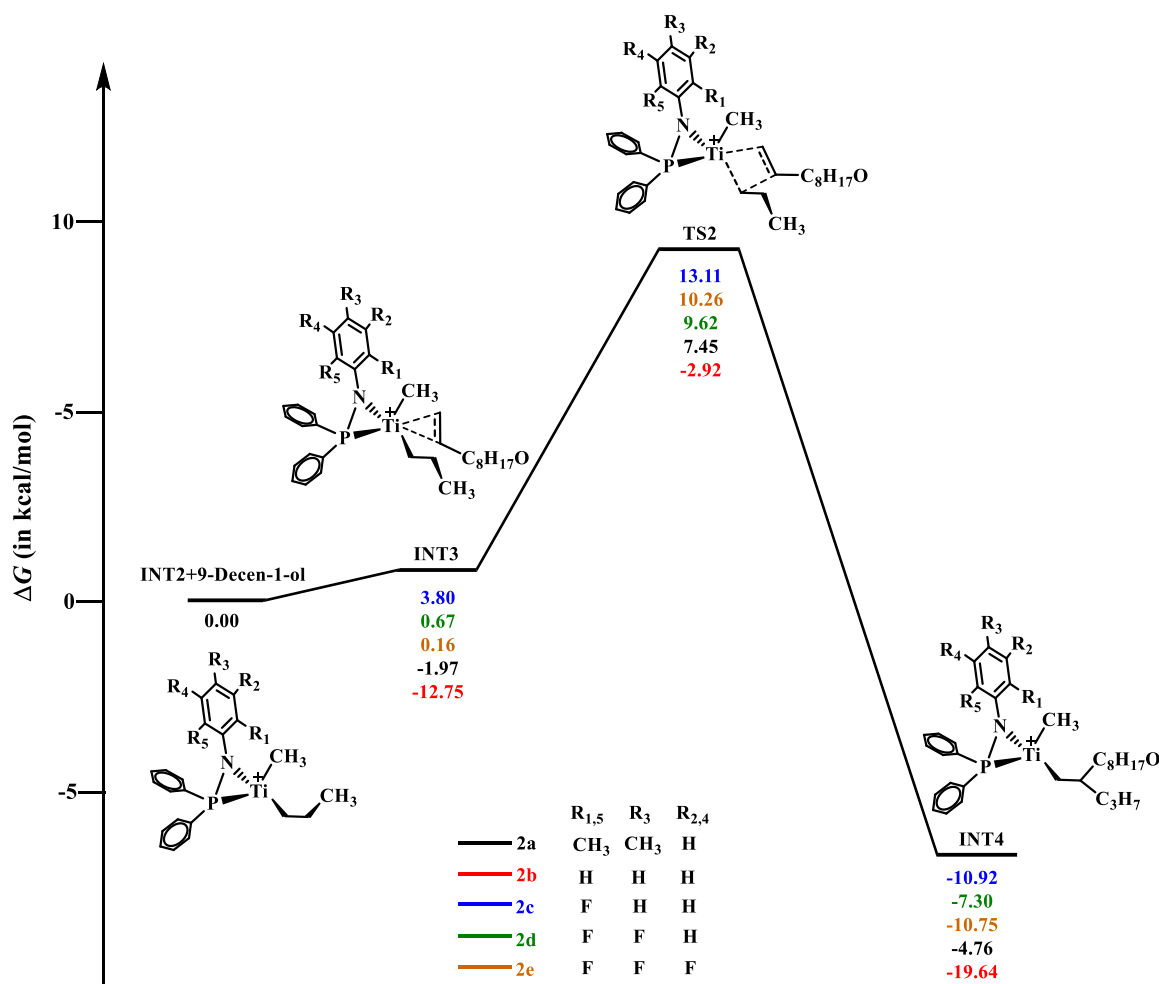


Figure 4. Computed energy profiles (free energy in kcal/mol) for insertion of first 1-octene monomer into INT2.

from HOMO to LUMO energy level. The computational results implied that the energies of HOMO and LUMO can be altered by changes of ancillary ligands, which can reflect the stability of the complexes. The stability of complexes followed the trend  $2b > 2c > 2e > 2d > 2a$ . It can be seen from the picture 1b [the active centers (2a–2e) that has initiated the

first step of ethylene reaction] that the energy gaps show similar regularity. With the introduction of electron-withdrawing group in the ligand structure of the complexes, the corresponding stability of the catalyst was significantly increased.



**Figure 5.** Computed energy profiles (free energy in kcal/mol) for insertion of the first 9-decen-1-ol into INT2.

To reveal the catalyst capability toward ethylene (homo) copolymerization and gain insights into the 2a–2e promoted copolymerization, DFT calculations were utilized to estimate the state energy and the energy barriers. The insertion of the first ethylene monomer into the Ti–C bond of the complexes was calculated. The computed energy profiles are shown in Figure 2. The energy barriers during the insertion process for ethylene were calculated as 9.70, 8.47, 8.69, 8.23, and 8.50 kcal/mol (2a, 2b, 2c, 2d, and 2e), respectively. Lower energy barrier suggests that the complexes display better polymerization ability. This calculation result indicates that the insertion ability of the first ethylene monomer into the Ti–CH<sub>3</sub> bond of 2a–2e complexes bearing electron-withdrawing (fluorine atom) is higher than that with electron-donating (CH<sub>3</sub>) substituents.

To investigate the origin of the observed activity discrepancy during chain propagation, the continuous insertion of the second ethylene was calculated (Figure 3). The energy barriers for the second ethylene insertion process were calculated as 3.71, 10.86, 2.91, 1.21, and 0.66 kcal/mol (2a, 2b, 2c, 2d, and 2e), respectively. Compared with the first ethylene insertion, the barrier value for the migratory insertion of the second ethylene monomer is significantly lower. The results reasonably explained that the complexes bearing electron-withdrawing exhibited highly favorable reactivity. Complexes 2c–2e exhibited a positive correlation between more fluorine substituents and higher activity, in the order 2e > 2d > 2c. The

calculated results are consistently well with the results of the polymerization experiments in the catalytic activity.

A comparison of the calculated insertion profiles for ethylene/1-octene copolymerization is shown in Figure 4. The calculated results revealed that the energy barrier height for the insertion of octene has significant discrepancy among the systems of 2a–2e. It indicated that the complexes with F/CH<sub>3</sub> groups (2a vs 2c vs 2d vs 2e = 5.70 vs 9.08 vs 7.29 vs 7.99 kcal/mol) displayed lower energy barrier relative to the complexes without substituents (2b = 11.90 kcal/mol), suggesting that F/CH<sub>3</sub> improved the polymerization activity. Differently, with the increase of the number of fluorine atoms, the reaction barrier tends to decrease, suggesting that the introduction of F would reduce the barrier to insertion.

The calculated free-energy profiles are presented in Figure 5, and the barrier heights for the migratory insertion of the 9-decen-1-ol monomer are 9.42, 9.83, 9.31, 8.95, and 10.10 kcal/mol, respectively. The calculated results revealed that energy barriers among the complexes 2a–2e have no significant discrepancy, indicating that experimental results do not correlate well with theoretical calculation. However, the main trend that can be seen is that the introduction of the electron-withdrawing functional group (F) reduced the energy barrier (2a vs 2c vs 2d = 9.42 vs 9.31 vs 8.95 kcal/mol).

The introduction of an electron-withdrawing (F) group can decrease the electron density of Ti and become the electron-deficient active center. With the increase of Lewis acidity, it is

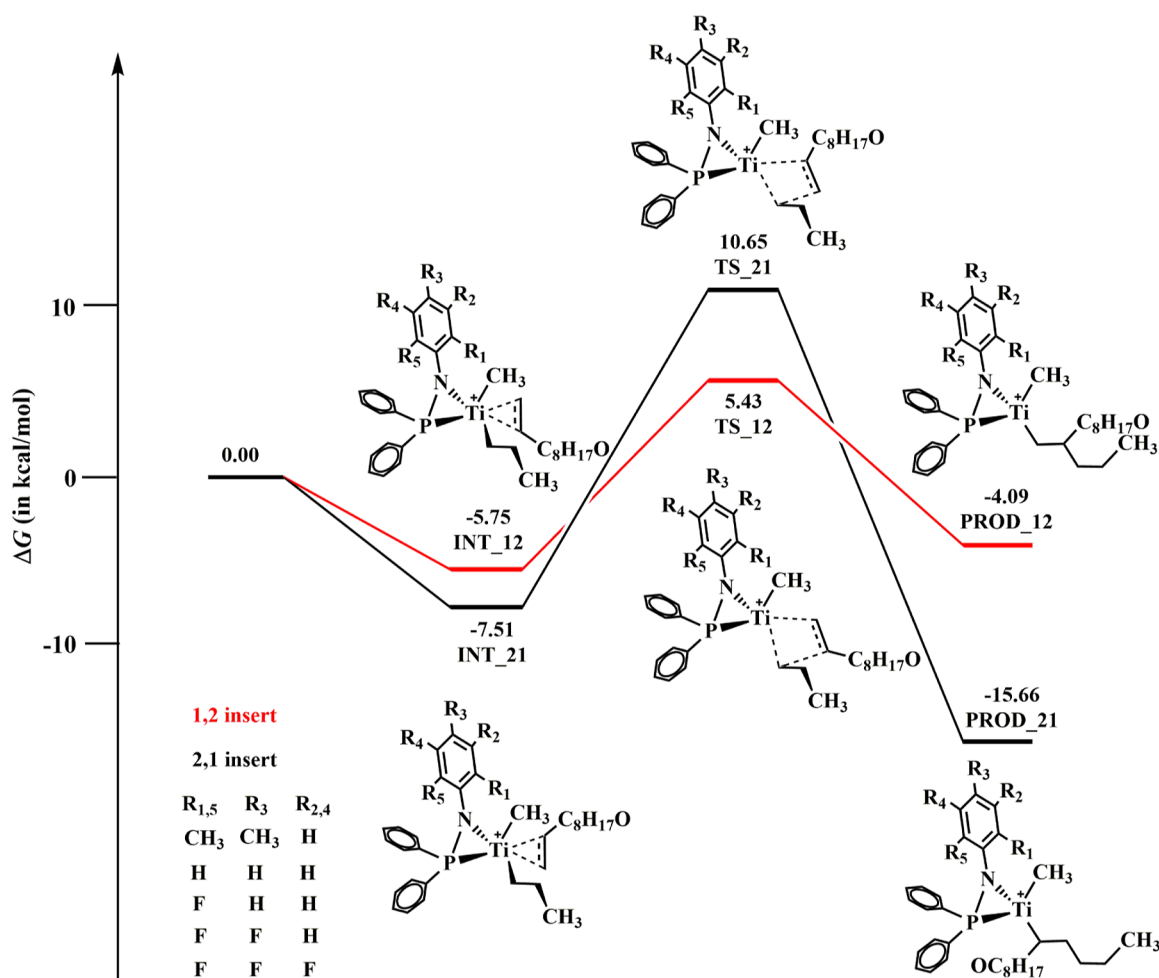


Figure 6. Computed energy profiles (free energy in kcal/mol) for the 9-decen-1-ol insertion.

easier to coordinate with the olefin monomer for polymerization. Accordingly, the enhanced electrophilicity of corresponding Ti complexes would promote olefin binding and activation for insertion, leading to an increase in the catalytic activity.

As shown in Figure 6, two different possible scenarios were considered for 9-decen-1-ol insertion in the chain initiation step. For each kind of insertion, 1,2-(primary) and 2,1-(secondary) insertion have been considered. The 2,1-insertion process (18.16 kcal/mol) has a higher free-energy barrier by more than 6.98 kcal/mol in comparison with the 1,2-insertion (11.18 kcal/mol), which suggested that the 1,2-insertion reaction is more preferable. This could be attributed to the strong steric repulsion between the olefin long chain of 9-decen-1-ol and the bulky ancillary ligands.

From the energy barriers calculated by DFT (Figure 7), the theoretical insertion value of 9-decen-1-ol can be deduced. The energy barrier difference was 2.03 kcal/mol (12.88 vs 10.85 kcal/mol) when the first elementary reaction monomer was ethylene, and the second elementary reaction monomers were ethylene and 9-decene-1-ol, respectively. The energy barrier difference was 4.05 kcal/mol (9.82 vs 5.77 kcal/mol), when the first to third step elementary reaction monomer was ethylene, and the fourth step elementary reaction monomers were ethylene and 9-decene-1-ol, respectively. The energy barrier difference was 0.93 kcal/mol (8.12 vs 7.19 kcal/mol), when the sixth step elementary reaction monomers were

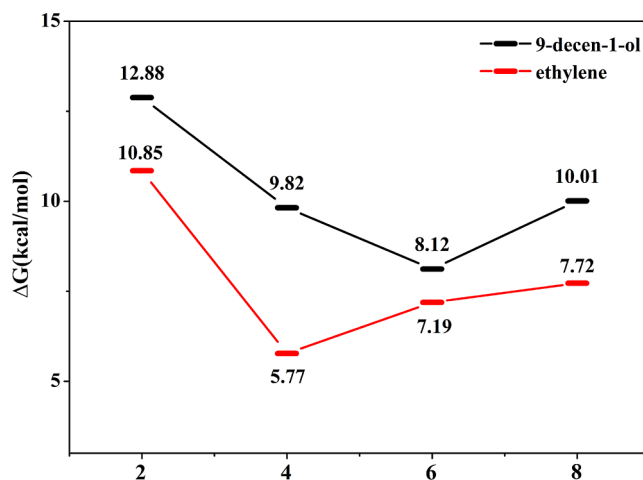
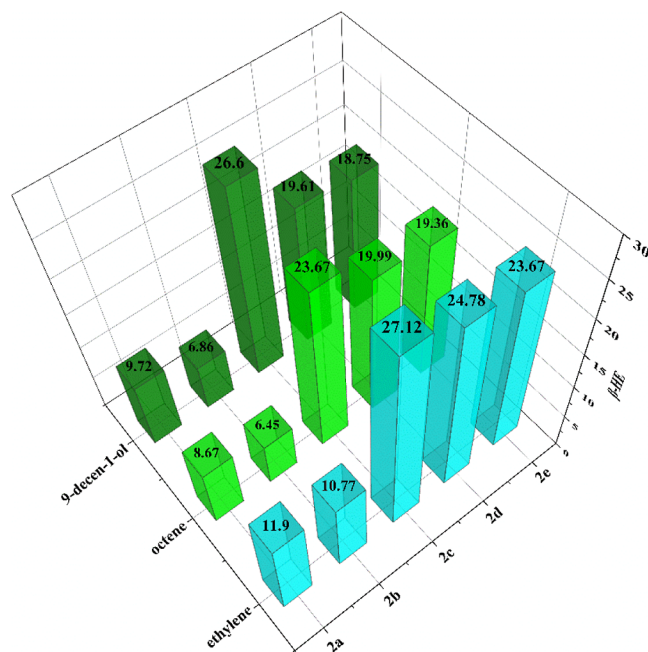


Figure 7. Energy profiles of second, fourth, sixth, and eighth steps of 9-decen-1-ol catalyzed by complex 2a.

ethylene and 9-decene-1-ol, respectively. The energy barrier difference was 2.29 kcal/mol (10.01 vs 7.72 kcal/mol) when the eighth step elementary reaction monomers were ethylene and 9-decene-1-ol, respectively. When the elementary reaction monomers in the sixth step were ethylene and 9-decen-1-ol, the energy barrier difference is the closest, and the probability of the 9-decen-1-ol monomer being inserted into the reaction

chain was the largest. On the above analysis, it can be inferred that the theoretical insertion value of 9-decen-1-ol was 16.7%.

The chain termination process has also been studied with DFT<sup>28</sup> (Figure 8). Three possible chain termination pathways



**Figure 8.** Calculated reaction profile for  $\beta$ -H elimination leading to chain termination.

were explored, where the ends of the molecular chain are ethylene, 1-octene, or 9-decen-1-ol. The termination barriers via the  $\beta$ -HE mechanism (ethylene) are 11.9, 10.77, 27.12, 24.78, and 23.67 kcal/mol for complexes 2a, 2b, 2c, 2d, and 2e, respectively. This shows that the ligands bearing different substituents have significant effect on the termination barrier. The electron-withdrawing F group increased the barrier, in accordance with expectation, in light of the large barrier of 27.12 kcal/mol encountered for 2c,  $\beta$ -HE may not occur very easily.<sup>16,19,29</sup> The increase in catalyst activity of introducing electron-withdrawing on ligands predicted by the DFT calculations agreed well with the experimental results. The termination barrier via the  $\beta$ -HE mechanism (1-octene/9-decen-1-ol) showed the same regularity: the introduction of electron-withdrawing F group increased the barrier. This work also follows our previous opinion<sup>16,29</sup> that with strong electron-withdrawing groups, the catalysts are good for olefin polymerization to show higher catalytic activity and more stable even at higher polymerization temperature, and the obtained polymer has higher-molecular weight. Recent many reports that Ni/Pd catalysts that have also exhibited the same polymerization behaviors are favorable for alpha-olefins and polar alpha-olefins (co)polymerization to show higher catalytic activity and have higher-molecular weight of obtained polyolefins.<sup>30,31</sup>

#### 4. CONCLUSIONS

In summary, a family of [N, P] Ti-based nonmetallocene complexes (2a–2e) were successfully developed. The synthesis method of complexes was simple, and the complexes displayed unexpected tolerance to polar groups. In the presence of polar 9-decen-1-ol, the complexes can effectively promote the

copolymerization of ethylene/1-octene/9-decen-1-ol, and copolymer with both the polymerization activity was up to  $1.04 \times 10^6$  gPolymer  $(\text{mol}\cdot\text{Ti})^{-1}\cdot\text{h}^{-1}$ , and the molecular weight as high as  $1.37 \times 10^6$  g/mol was obtained. Simultaneously, theoretical investigations exhibited that the activity of complexes in catalytic polymerization was significantly dependent on the substituents. The calculations confirmed that the introduction of F substituents into the ligands has a dramatic effect, which can obviously improve the activity of the complexes and the molecular weight of the polymer. The activity of complexes 2a–2e basically exhibited the following order: 2e > 2d > 2c > 2b > 2a. According to the calculated energy profiles, the experimentally displayed activity discrepancy was reasonably elucidated. It is noteworthy that the theoretical results could provide a valuable reference for the design of catalysts with excellent comprehensive performance.

#### AUTHOR INFORMATION

##### Corresponding Authors

**Ming Lei** – College of Chemistry, Beijing University of Chemical Technology, Beijing 100029, P. R. China; [orcid.org/0000-0001-5765-9664](https://orcid.org/0000-0001-5765-9664); Email: [leim@mail.buct.edu.cn](mailto:leim@mail.buct.edu.cn)

**Qigu Huang** – State Key Laboratory of Chemical Resource Engineering, Key Laboratory of Carbon Fiber and Functional Polymers, College of Material Science and Technology, Beijing University of Chemical Technology, Beijing 100029, P. R. China; [orcid.org/0000-0002-3367-3557](https://orcid.org/0000-0002-3367-3557); Email: [huangqg@mail.buct.edu.cn](mailto:huangqg@mail.buct.edu.cn)

##### Authors

**Jingjiao Liu** – State Key Laboratory of Chemical Resource Engineering, Key Laboratory of Carbon Fiber and Functional Polymers, College of Material Science and Technology, Beijing University of Chemical Technology, Beijing 100029, P. R. China

**Jiaojiao Zhang** – State Key Laboratory of Chemical Resource Engineering, Key Laboratory of Carbon Fiber and Functional Polymers, College of Material Science and Technology, Beijing University of Chemical Technology, Beijing 100029, P. R. China

**Min Sun** – The State Key Laboratory of Catalytic Materials and Reaction Engineering (RIPP, SINPPEC), Beijing 100083, P. R. China

**Hongming Li** – Petrochemical Research Institute, PetroChina, Beijing 102206, P. R. China

Complete contact information is available at:

<https://pubs.acs.org/10.1021/acsomega.3c09124>

##### Notes

The authors declare no competing financial interest.

#### ACKNOWLEDGMENTS

This study was financially supported by the State Key Laboratory of Catalytic Materials and Reaction Engineering (RIPP, SINPPEC. no.33600000-22-ZC0607-0012), the National Natural Science Foundation of China (no. U1462102 and 51603007), and the National Key Research and Development Program of China (no. 2021YFB2401501).

#### REFERENCES

(1) Carrow, B. P.; Nozaki, K. Transition-Metal-Catalyzed Functional Polyolefin Synthesis: Effecting Control through Chelating Ancillary

- Ligand Design and Mechanistic Insights. *Macromolecules* **2014**, *47* (8), 2541–2555.
- (2) Stürzel, M.; Mihan, S.; Mülhaupt, R. From Multisite Polymerization Catalysis to Sustainable Materials and All-Polyolefin Composites. *Chem. Rev.* **2016**, *116* (3), 1398–1433.
- (3) Keyes, A.; Basbug Alhan, H. E.; Ordonez, E.; Ha, U.; Beezer, D. B.; Dau, H.; Liu, Y. S.; Tsogtgerel, E.; Jones, G. R.; Harth, E. Olefins and Vinyl Polar Monomers: Bridging the Gap for Next Generation Materials. *Angew. Chem., Int. Ed.* **2019**, *58* (36), 12370–12391.
- (4) Franssen, N. M. G.; Reek, J. N. H.; de Bruin, B. Synthesis of Functional ‘Polyolefins’: State of the Art and Remaining Challenges. *Chem. Soc. Rev.* **2013**, *42* (13), 5809–5832.
- (5) Boffa, L. S.; Novak, B. M. Copolymerization of Polar Monomers with Olefins Using Transition-Metal Complexes. *Chem. Rev.* **2000**, *100* (4), 1479–1494.
- (6) Nakamura, A.; Ito, S.; Nozaki, K. Coordination-Insertion Copolymerization of Fundamental Polar Monomers. *Chem. Rev.* **2009**, *109* (11), 5215–5244.
- (7) Chen, E. Y. X. Coordination Polymerization of Polar Vinyl Monomers by Single-Site Metal Catalysts. *Chem. Rev.* **2009**, *109* (11), 5157–5214.
- (8) Terao, H.; Ishii, S.; Mitani, M.; Tanaka, H.; Fujita, T. Ethylene/Polar Monomer Copolymerization Behavior of Bis(phenoxy-imine)Ti Complexes: Formation of Polar Monomer Copolymers. *J. Am. Chem. Soc.* **2008**, *130* (52), 17636–17637.
- (9) Chen, Z.; Li, J. F.; Tao, W. J.; Sun, X. L.; Yang, X. H.; Tang, Y. Copolymerization of Ethylene with Functionalized Olefins by [ONX] Titanium Complexes. *Macromolecules* **2013**, *46* (7), 2870–2875.
- (10) Zhang, Y.; Mu, H.; Pan, L.; Wang, X.; Li, Y. Robust Bulky [P,O] Neutral Nickel Catalysts for Copolymerization of Ethylene with Polar Vinyl Monomers. *ACS Catal.* **2018**, *8* (7), 5963–5976.
- (11) Hong, M.; Wang, Y. X.; Mu, H. L.; Li, Y. S. Efficient Synthesis of Hydroxylated Polyethylene via Copolymerization of Ethylene with 5-Norbornene-2-methanol using  $\beta$ -(enaminoketonato)titanium Catalysts. *Organometallics* **2011**, *30* (17), 4678–4686.
- (12) Mitsushige, Y.; Yasuda, H.; Carrow, B. P.; Ito, S.; Kobayashi, M.; Tayano, T.; Watanabe, Y.; Okuno, Y.; Hayashi, S.; Kuroda, J.; Okumura, Y.; Nozaki, K. Methylene-Bridged Bisphosphine Monoxide Ligands for Palladium-Catalyzed Copolymerization of Ethylene and Polar Monomers. *ACS Macro Lett.* **2018**, *7* (3), 305–311.
- (13) Zhang, W.; Waddell, P. M.; Tiedemann, M. A.; Padilla, C. E.; Mei, J.; Chen, L.; Carrow, B. P. Electron-Rich Metal Cations Enable Synthesis of High Molecular Weight, Linear Functional Polyethylenes. *J. Am. Chem. Soc.* **2018**, *140* (28), 8841–8850.
- (14) Zhao, X.; Li, H.; Liu, Y.; Ma, Y. Substituent Effects on Propylene Polymerization in Cyclic Bis(phenoxyaldimine) Titanium Catalysts. *Macromolecules* **2020**, *53* (24), 10803–10812.
- (15) Michalak, A.; Ziegler, T. DFT Studies on the Copolymerization of  $\alpha$ -Olefins with Polar Monomers: Comonomer Binding by Nickel- and Palladium-Based Catalysts with Brookhart and Grubbs Ligands. *Organometallics* **2001**, *20* (8), 1521–1532.
- (16) Huang, Q. G.; Huang, H. B.; Guo, J. P.; Fan, M.; Li, F. J.; Cheng, L.; Liu, Z.; Liu, W.; Yang, W. T. Non-metallocene catalyst with full hetero-member ring and its’ preparation method and application. CN 201310108975.1 A, 2013.
- (17) Ehm, C.; Budzelaar, P. H. M.; Busico, V. Calculating accurate barriers for olefin insertion and related reactions. *J. Organomet. Chem.* **2015**, *775* (1), 39–49.
- (18) Walker, W. K.; Anderson, D. L.; Stokes, R. W.; Smith, S. J.; Michaelis, D. J. Allylic Aminations with Hindered Secondary Amine Nucleophiles Catalyzed by Heterobimetallic Pd-Ti Complexes. *Org. Lett.* **2015**, *17*, 752–755.
- (19) Wang, J.; Nan, F.; Guo, J. P.; Wang, J.; Shi, X. H.; Huang, H. B.; Huang, Q. G.; Yang, W. T. Copolymers of Ethylene and Vinyl Amino Acidic Ester with High Molecular Weight Prepared by Non-metallocene Catalysts. *Catal. Lett.* **2016**, *146* (3), 609–619.
- (20) Wang, X.; Lin, F.; Qu, J.; Hou, Z.; Luo, Y. DFT Studies on Styrene Polymerization Catalyzed by Cationic Rare-Earth-Metal Complexes: Origin of Ligand-Dependent Activities. *Organometallics* **2016**, *35* (18), 3205–3214.
- (21) Ciancaleoni, G.; Fraldi, N.; Cipullo, R.; Busico, V.; Macchioni, A.; Budzelaar, P. H. M. Structure/Properties Relationship for Bis(phenoxyamine)Zr(IV)-Based Olefin Polymerization Catalysts: A Simple DFT Model To Predict Catalytic Activity. *Macromolecules* **2012**, *45* (10), 4046–4053.
- (22) Barron, A. R. New Method for the Determination of the Trialkylaluminum Content in Alumoxanes. *Organometallics* **1995**, *14* (7), 3581–3583.
- (23) Chien, J. C. W.; Salajka, Z.; Dong, S. Syndiospecific Polymerization of Styrene. 3. Catalyst Structure. *Macromolecules* **1992**, *25* (12), 3199–3203.
- (24) Zhu, F. M.; Huang, Q. G.; Lin, S.-An. Syntheses of multi-stereoblock polybutene-1 using novel monocyclopentadienyltitanium and modified methylaluminoxane catalysts. *J. Polym. Sci., Part A: Polym. Chem.* **1999**, *37*, 4497–4501.
- (25) Coates, G. W. Precise Control of Polyolefin Stereochemistry Using Single-Site Metal Catalysts. *Chem. Rev.* **2000**, *100*, 1223–1252.
- (26) Sahu, H.; Panda, A. N. Computational Study on the Effect of Substituents on the Structural and Electronic Properties of Thiophene-Pyrrole-Based  $\pi$ -Conjugated Oligomers. *Macromolecules* **2013**, *46* (3), 844–855.
- (27) Park, D. A.; Byun, S.; Ryu, J. Y.; Lee, J.; Lee, J.; Hong, S. Abnormal N-Heterocyclic Carbene-Palladium Complexes for the Copolymerization of Ethylene and Polar Monomers. *ACS Catal.* **2020**, *10* (10), 5443–5453.
- (28) Woo, T. K.; Fan, L.; Ziegler, T. A Density Functional Study of Chain Growing and Chain Terminating Steps in Olefin Polymerization by Metallocene and Constrained Geometry Catalysts. *Organometallics* **1994**, *13* (6), 2252–2261.
- (29) Huang, Q. G.; Fu, Y.; Shi, Z. H.; Zhang, S. M.; Wang, Q. C.; Yu, H. C.; Yang, W. T.; Metallocene catalyst and its’ preparation method and application. CN 201810590083.2 A, 2018.
- (30) Hu, X. Q.; Kang, X. H.; Jian, Z. B. Suppression of Chain Transfer at High Temperature in Catalytic Olefin Polymerization. *Angew. Chem., Int. Ed.* **2022**, *61*, No. e202207363.
- (31) Zou, C.; Si, G. F.; Chen, C. L. A general strategy for heterogenizing olefin polymerization catalysts and the synthesis of polyolefins and composites. *Nat. Commun.* **2022**, *13*, 1954.